INCLUSIVE (^{3}He, t) REACTION ON NUCLEI

P. Fernández de Córdoba*,
E. Oset**,M.J. Vicente-Vacas**

* *Departamento de Matemática Aplicada*
Universidad Politécnica de Valencia, 46022 Valencia (Spain)
** *Departamento de Física Teórica and IFIC*
Centro Mixto Universitat de Valencia CSIC, 46100 Burjassot (Valencia), Spain.

Abstract

We study the channels which contribute to the $(^3He, t)$ reaction in the region of excitation of the Δ resonance. We show that the shift of the delta peak in nuclei is due to a collaboration of many processes: delta excitation in the projectile, quasielastic collisions, virtual pion absorption and coherent pion production.

1 Introduction

The $(^3He,t)$ reaction in nuclei in the region of the Δ excitation is rather complex and there are many different channels which collaborate and sometimes compete, in producing the observed experimental strength. As a consequence it has resisted a simple theoretical interpretation.

An overall view of the $(^3He,t)$ process on proton, deuteron and ^{12}C targets is shown in fig. 1. Some features are worth noting with respect to this figure. The deuteron spectrum is clearly shifted towards higher t energies with respect to the spectrum for p targets. The peak is not much shifted but much strength accumulates now at lower excitation energies. On the other hand at the high side of the t spectrum some strength accumulates which is clearly attributable to quasielastic collisions of the type $He\ n \longrightarrow t\ p$ and which do not occur with the p targets. A smooth extrapolation of this part of the spectrum in the d case below the Δ excitation peak also shows that the new strength of the d excitation function with respect to the proton can not be attributed to these quasielastic collisions. On the other hand the peak of the distribution in ^{12}C is clearly shifted toward higher t energies and a considerable amount of strength is also shifted. However, contrary to the case of the deuteron, the quasielastic peak is so large that one immediately realizes that its extrapolation below the apparent delta peak must have much to do with the strength of this peak. Hence any serious attempt to explain the inclusive spectra shown in fig. 1 must take the quasielastic channels into consideration.

There are several recent theoretical and experimental developments on the delta excitation with hadronic probes that have increased considerably our understanding of these reactions. Exclusive experiments looking for detailed channels [1], [2] have brought valuable information to clarify the important issues. The $(^3He,t)$ reaction on p has been nicely described in ref. [3] [4] [5] although using different approaches.

The deuteron spectrum finds a simple interpretation by considering the delta excitation in the projectile (DEP) in addition to the delta excitation in the target (DET) [3] which was dominant in the reaction on the proton.

The idea of coherent pion production has also stimulated some work [6], [7],[8], and it appears to be one of the important factors in the interpretation of the shift of the peak position in nuclei. Experiments devoted to provide the absolute cross sections for coherent pion production in nuclei are under way and some preliminary results are already available in refs. [9], [10].

In this work we will address the inclusive $(^3He,t)$ reaction in nuclei. As mentioned before, many channels are involved, apart from those already present in the deuteron case. All the incoherent channels are considered simultaneously using a Monte Carlo (MC) simulation procedure and the coherent channel, calculated separately, is also incorporated to the model.

We will consider the following channels: quasielastic $^3HeN \longrightarrow tN$ collisions; multistep quasielastic collision, for instance $^3HeN \longrightarrow^3 He(t)N$ followed by $^3He(t)N \longrightarrow tN$; two steps quasielastic with $^3He(t)$ break up in the

intermediate states; virtual pion production followed by two (or three body) pion absorption (the virtual pion is in practice substituted by the spin-isospin effective interaction); incoherent inclusive π^+ and π^o production and coherent pion production.

The model for the coherent π-production is based in the work of ref. [18] where the cross section for coherent pion production in the $^3He + ^{12}C \longrightarrow t + ^{12}C + \pi^+$ was calculated. The Δ peak of the energy distribution is considerably shifted with respect to the peak in the $p(^3He, t)\Delta^{++}$ reaction. The coherent pions represent a sizeable fraction of all pions produced and are an essential ingredient in the interpretation of the Δ peak in the inclusive $(^3He, t)$ reaction in ^{12}C.

In the case of incoherent pion production we use the model for the elementary $N(^3He, t)N\pi$ reaction in [3] and incorporate the medium effects. We also consider the $N(^3He,^3 He)N\pi$ reaction based in the model of ref. [11], followed by a $^3He + n \longrightarrow t + p$ collision, or the $N(t, t)N\pi$ reaction preceded by a $^3He + n \longrightarrow t + p$ collision. In the $N(^3He,^3 He)N\pi$ (or $N(t, t)N\pi$) reaction the DEP mechanism is very important whereas the DET mechanism provides a small contribution. Also, the shapes of the two mechanisms are completely different and the peak of the DEP mechanism is shifted by about 140 MeV towards higher energies of the outgoing ^3He with respect to the peak of the DET mechanism. The cross section of this $N(^3He,^3 He)N\pi$ reaction is also much larger than in the $N(^3He, t)N\pi$ reaction [11].

The rest of the processes involved are described below.

2 Description of the Simulation Procedure

The ^3He nuclei are thrown with random impact parameter $\vec{b}$, uniformly distributed in the circle $|\vec{b}| < b_{max}$, where b_{max} is a distance beyond which there is no interaction between the incoming ^3He and the nuclear target. The ^3He nuclei are then moved along the z-axis starting from a point $-z_{min}$ such that $z_{min}^2 + b^2 = b_{max}^2$.

The incoming ^3He is moved in steps of size δz and, in every step, we check whether there is interaction with the nuclear target.

Assume that P_i is the probability per unit length associated to the $i-th$ channel of interaction. The interval of length δz is chosen such that $\sum_{i=1}^{N} P_i \delta z$ is much smaller than the unity, (N is the number of interaction channels). A random number $x \in [0,1[$ is generated.

There are two possibilities:

1) $(P_1 + P_2 + ... + P_N)\delta z \leq x < 1$. Then, the ^3He has not interacted in this step.

2) $(P_1 + ...P_{i-1})\delta z < x < (P_1 + ... + P_i)\delta z$. In this case the ^3He follows the $i-th$ interaction channel, for instance collides quasielastically and changes energy and direction.

This algorithm is iterated until either the $^3He(t)$ is broken or gets out from the target nucleus. When it is a tritium nucleus what gets out from the target its energy and angle are stored.

At the end of the simulation the total and differential cross sections of the $(^3He,t)$ reaction are evaluated. For instance the total cross section is given by [12]:

$$\sigma_t = \pi b_{max}^2 . \frac{N}{N_T} \tag{1}$$

Where N_T is the total number of beam particles thrown and N is the number of events in which a tritium was emitted.

To evaluate the angular distributions we proceed in the following way: the range of the scattering angle is divided in N_μ equal angular intervals (angular channel). If μ is the cosinus of the scattering angle of the outgoing tritium we associate it to a discrete value, the medium point of the interval in which μ is included [12]:

$$\mu \longrightarrow \mu_k = (k - \frac{1}{2})\delta\mu - 1 \tag{2}$$

where

$$\delta\mu = \frac{2}{N_\mu}, k = 1 + [\frac{\mu + 1}{\delta\mu}] \tag{3}$$

if n_k tritiums are stored in the $k-th$ angular channel, we have for the angular distribution the following expressions

$$N = \sum_{k=1}^{N_\mu} n_k$$

$$\sigma_t = \pi b_{max}^2 \frac{\sum n_k}{N_T} \tag{4}$$

$$\frac{d\sigma_t}{d\Omega}|_k = \pi b_{max}^2 \frac{n_k}{N_T} \frac{1}{2\pi\delta\mu} =$$

$$= \frac{n_k}{N_T} \frac{N_\mu}{4} b_{max}^2$$

For the energy or double differential distributions we proceed analogously.

3 Probabilities of the interaction channels

3.1 Quasielastic collisions

In the $(^3He, t)$ reaction on nuclei many quasielastic processes are involved:
- One step quasielastic collisions
  $^3He + n \longrightarrow t + p$
- Multistep quasielastic collisions, for instance
$i)$ $^3He + n \longrightarrow t + p$ followed by $t + N \longrightarrow t + N$
$ii)$ $^3He + N \longrightarrow ^3He + N$ followed by $^3He + n \longrightarrow t + p$

In this model we consider simultaneously these processes including all of them in the MC simulation code. For this purpose we need to know the total cross sections and the angular and energy distributions of all those elementary processes. We take this information directly from the experiment [13].

Using the available experimental data [13] we parametrize $\frac{d\sigma}{dt}$ as a function of the Mandelstam variables s and t for the following processes:

$$p + ^3He \longrightarrow p + ^3He$$

$$p + t \longrightarrow p + t \tag{5}$$

$$p + t \longrightarrow n + ^3He$$

Using the parametrizations of $\frac{d\sigma}{dt}(s,t)$ for the free processes we can evaluate the probabilities for these channels inside a nucleus. As an example we will show in detail the calculation for the case of the $^3He + n \longrightarrow t + p$ reaction. The associated cross section for one neutron is given by

$$\frac{d^2\sigma}{dE_t d\Omega_t} = \frac{M}{4\pi^3} |\vec{p}_{He}||\vec{p}_t||\vec{p}_p| \frac{d\sigma}{dt} \sum_n \int_{-1}^{1} dcos\theta |\tilde{\psi}_n(\vec{q} - \vec{p}_p)|^2 \tag{6}$$

where $\vec{q} = \vec{p}_{He} - \vec{p}_t$, M the nucleon mass, and θ is the angle between $\vec{q}$ and $\vec{p}_p$, see fig. 2. The sum in eq. (6) runs over the nuclear states occupied by the neutrons of the ^{12}C and $\tilde{\psi}_n(\vec{q}-\vec{p}_p)$ is the Fourier transform of the neutron wave function in the state n, i.e.

$$\psi_n(\vec{q}-\vec{p}_p) \equiv \int d^3\vec{x} e^{-i\vec{p}_p\vec{x}} e^{i\vec{q}\vec{x}} \psi_n(\vec{x}) \tag{7}$$

Using a harmonic oscillator model for these wave functions

$$\psi_{1s}(r) = (\frac{4\alpha^3}{\sqrt{\pi}})^{1/2} e^{-1/2\alpha^2 r^2} Y_{oo}(\Omega)$$

$$\psi_{1p}(r) = (\frac{8\alpha^5}{3\sqrt{\pi}})^{1/2} r e^{-1/2\alpha^2 r^2} Y_{1m}(\Omega) \tag{8}$$

we can evaluate analytically the eq. (6)
Using in eq. (7) the decomposition of the plane wave in spherical harmonics we can write

$$\sum_n |\tilde{\psi}_n(\vec{q}-\vec{p}_p)|^2 = 4\pi\{2I_{10}^2(\vec{q}-\vec{p}_p) + 4I_{11}^2(\vec{q}-\vec{p}_p)\} \tag{9}$$

where

$$I_{nl}(\vec{q}) = \int_0^\infty r^2 dr j_l(qr) R_{nl}(r) \tag{10}$$

With $R_{nl}(r)$ the radial part of the wave functions in eq. (8) and $j_l(qr)$ the Bessel function of order l. Using the eq. A-7 in ref. [14] we get

$$I_{10}(q) = (\frac{2\sqrt{\pi}}{\alpha^3})^{1/2} e^{-q^2/2\alpha^2}$$

$$I_{11}(q) = (\frac{4\sqrt{\pi}}{3\alpha^5})^{1/2} q e^{-q^2/2\alpha^2} \tag{11}$$

and then

$$\sum_n \int_{-1}^{1} dcos\theta |\tilde{\psi}_n(\vec{q}-\vec{p}_p)|^2 =$$

$$= \frac{16\pi^{3/2}}{\alpha^3}\{M(p_p,q,\alpha^2) + \frac{4}{3}N(p_p,q,\alpha^2)\} \tag{12}$$

where

$$M(p,q,\alpha^2) \equiv \frac{\alpha^2}{2pq}\{e^{-(p-q)^2/\alpha^2} - e^{-(p+q)^2/\alpha^2}\}$$

$$N(p,q,\alpha^2) \equiv \frac{\alpha^2}{2pq}\{e^{-(p-q)^2/\alpha^2}[1 + \frac{(p-q)^2}{\alpha^2}] - \tag{13}$$

$$-e^{-(p+q)^2/\alpha^2}[1+\frac{(p+q)^2}{\alpha^2}]\}$$

We take $\alpha^2 = 0.37 fm^{-2}$ for the ^{12}C.
In this approach we have not imposed the Pauli blocking in the outgoing nucleon but we have checked that in the kinematic conditions of the experiment (particularly below the Δ peak) this correction is small. Finally, the probability per unit length is obtained by multiplying the calculated cross section by the density of neutrons.

Alternatively, one could use a simpler picture of the nucleus and assume that the nucleons move in a local fermi sea. Then integrate over initial nucleons –or take an average nucleon– do simple kinematics and exclude the events that are forbidden by the Pauli blocking in the outgoing nucleon.

The probability of this reaction per unit length, needed in the Monte Carlo simulation is obtained by multiplying eq. (6) by $\rho(\vec{r})/A$, with $\rho(\vec{r})$ the density of ^{12}C and A its mass number.

3.2 Virtual pion absorption

One of the processes which contributes to the inclusive reaction $(^3He, t)$ on nuclei is the virtual pion absorption. Its probability is proportional to the imaginary part of the selfenergy diagrams of fig. 3, which account for the reactions $(^3He, tNN)$ and $(^3He, tNNN)$ (absorption of the virtual pion by two and three nucleons respectively). The double differential cross section associated to the process depicted in fig. 3 is given by

$$\frac{d^2\sigma}{dE_t d\Omega_t} = -2\frac{M_{He}}{|\vec{k}|}\frac{1}{(2\pi)^3}\int d^3r\theta(q^0)2(\frac{f}{\mu})^2$$

$$\vec{q}^{\,2}[D(q)]^2\frac{M_t}{E_t(\vec{k}-\vec{q})}|Im\Pi^{abs}(q,\rho(\vec{r}))|_{q^0=k^0-E_t(\vec{k}-\vec{q})} \qquad (14)$$

where $k = (k^0, \vec{k})$ is the momentum of the incoming ^3He, f is the πNN coupling constant ($f^2/4\pi = 0.08$) and μ the pion mass. $Im\Pi^{abs}(\vec{q}, \rho(\vec{r}))$ is the imaginary part of the pion self-energy related to pion absorption [15] and $D(q)$ the pion propagator. In ref [15] the pion selfenergy, Π, was evaluated microscopically and the different sources of $Im\Pi$ were separated. Each one of these parts was associated to a physical channel, quasielastic or absorption. Here, only the absorption part of Π is considered. The same steps below using the quasielastic part of the pion selfenergy account for the $^3He + N \longrightarrow t + N + \pi$ reaction. In the next section we discuss further details on this channel.

If we split the pion selfenergy in s-wave and p-wave parts:

$$\Pi^{abs}(q,\rho(\vec{r})) = \Pi^{(s)}(q,\rho(\vec{r})) + \vec{q}^{\,2}\bar{\Pi}^{(p)}(q,\rho(\vec{r})) \qquad (15)$$

and incorporate the medium corrections as in [15], we can write

$$\frac{d^2\sigma}{dE_t d\Omega_t} = -2\frac{M_{He}}{|\vec{k}|}\frac{1}{(2\pi)^3}\int d^3r\theta(q^0)2(\frac{f}{\mu})^2 F_{He,t}^2(q)$$

$$\frac{M_t}{E_t(\vec{k}-\vec{q})}\{\frac{Im\Pi^{(s)}(q,\rho(\vec{r}))}{|1-U(q)V_l(q)|^2}(-q^2)[D(q)]^2 + \tag{16}$$

$$[\frac{V_l'^2}{|1-U(q)V_l(q)|^2} + \frac{2V_t'^2}{|1-U(q)V_t(q)|^2}]Im\bar{\Pi}^{(p)}(q,\rho(\vec{r}))\}$$

where

$$V_l = (\frac{f}{\mu})^2 V_l' \ , \ V_t = (\frac{f}{\mu})^2 V_t' \tag{17}$$

with

$$V_l' = \frac{-q^2}{q^{02}-\vec{q}^2-\mu^2}F_\pi(q)^2 + g'$$

$$V_t' = \frac{-q^2}{q^{02}-\vec{q}^2-m_\rho^2}F_\rho(q)^2 C_\rho + g' \tag{18}$$

where $F_\pi(q), F_\rho(q), C_\rho$ and g' are defined in [3]. $U(q)$ is the Lindhard function[16] that includes both the nucleon and delta contributions and $F_{He,t}(q)$ is the $(^3He,t)$ transition form factor [3].

For the pion selfenergy we use the results of ref. [15].The s-wave contribution is negligible for the pion momenta that we are interested in. At energies of the pion around the Δ region, $\bar{\Pi}^{(p)}$ is dominated by the Δ excitation, which is proportional to the Δ propagator

$$G_\Delta = \frac{1}{\sqrt{s}-M_\Delta+\frac{i}{2}\tilde{\Gamma}_\Delta-\Sigma_\Delta} \tag{19}$$

where $\tilde{\Gamma}_\Delta$ is the free Δ width with Pauli corrections and Σ_Δ its selfenergy [15].

For the real part of the Δ selfenergy we take [15]

$$Re\Sigma_\Delta = -53\rho(\vec{r})/\rho_0[MeV] \tag{20}$$

where $\rho(\vec{r})$ is the nuclear density and ρ_0 the nuclear matter density ($\rho = 0.17fm^{-3}$).

For the imaginary part of the Δ selfenergy we take [15]

$$Im\Sigma_\Delta = Im\Sigma^q + Im\Sigma_\Delta^2 + Im\Sigma_\Delta^3 \tag{21}$$

where $Im\Sigma_\Delta^2$ is associated to the resonant part in the two body absorption and $Im\Sigma_\Delta^3$ is associated to the three body absorption. $\tilde{\Gamma}_\Delta/2$ and $Im\Sigma^q$ are associated to the quasielastic channels. At lower excitation energies, non resonant terms in the pion selfenergy become important, and around excitation

energies close to the pion mass they provide a contribution to Π^{abs} about three times larger than the Δ excitation contribution alone. This is important to note because in the present process the contribution to the $(^3He,t)$ reaction from virtual pion absorption peaks around excitation energies close to the pion mass. Two factors are responsible for this feature: the $(^3He,t)$ transition form factor and the fact that these virtual pions have an energy $q^0 \approx m_\pi$ but a sizeable momentum q, unlike real pions which have zero momentum at this energy, and $\bar{\Pi}^{(p)}$ is proportional to $\vec{q}^2$.

We should note that in the approaches of [4, 5, 8] virtual pion absorption is implicitly incorporated in terms of the imaginary part of the Δ selfenergy in the medium used there, but only the part corresponding to Δ excitation, i.e., the non resonant terms discussed above are not included.

The probability of this reaction per unit length, needed in the Monte Carlo simulation, is given by eq.(16) omitting the d^3r integration.

3.3 Pion production

In the $(^3He,t)$ reaction on nuclei several processes with π-production are involved.

- One step π-production $^3He + N \longrightarrow t + N + \pi$
- Multistep π-production, for instance

i)

$$^3He + N \longrightarrow \{ \begin{matrix} ^3He \\ t \end{matrix} \} + N$$

$$+$$

$$N \longrightarrow t + N + \pi$$

where we have a quasielastic collision followed by a π production process.

ii)

$$^3He + N \longrightarrow \{ \begin{matrix} ^3He \\ t \end{matrix} \} + N + \pi$$

$$+$$

$$N \longrightarrow t + N$$

where we have a π production process followed by a quasielastic collision.

The model for the π-production processes in the $(^3He,t)$ reaction, on protons and neutrons, is described in [3]. The nuclear medium corrections to these channels are incorporated as discussed in the previous section. The π-production processes in the $(^3He,^3He)$ reaction, on protons and neutrons, are studied in [11]. For the (t,t) reaction on protons or neutrons we take the

(^3He,^3He) cross sections on neutrons or protons respectively. In both cases the calculations include the Δ excitation in the target and Δ excitation in the projectile mechanisms and the $\pi - N$ s-wave interaction.

3.4 Intermediate excited states

We also consider processes with excited ^3He or t as intermediate states, for instance

$$^3He + N \longrightarrow \{ \begin{matrix} ^3He^* \\ t^* \end{matrix} \} + N \tag{22}$$

$$+$$

$$N \longrightarrow t + N$$

We represent these diagrams in fig. 4.

To evaluate the double differential cross section for the process depicted in fig. 4 we use a closure sum approximation, assuming an average value for the energy of the different intermediate states, and we use the relation between the transition amplitude and the differential cross section $\frac{d\sigma}{dt}$ for the $p + t \longrightarrow n + ^3He$ reaction. Then, we can relate the double differential cross section for the process depicted in fig. 4 with $\frac{d\sigma}{dt}$ for the $p + t \longrightarrow n + ^3He$ process:

$$\frac{d^2\sigma}{dE_t d\Omega_t} = \frac{8}{\pi} \frac{k p_t^3}{M_{He} M_t} \int d^3r \int \frac{d^4q}{(2\pi)^4} \theta(q^0)\theta(q'^0)$$

$$ImU_N ImU_N(q')|\frac{M_{He}}{\tilde{E}^*_{He}} \frac{1}{k^0 - q^0 - \tilde{E}^*_{He} - iIm\Sigma_{He^*}}|^2 \tag{23}$$

$$\{(\frac{d\sigma}{dt}(t=0))^{1/2}(\frac{d\sigma}{dt}(t=(q+q')^2))^{1/2} -$$

$$-(\frac{d\sigma}{dt}(t=q^2))^{1/2}(\frac{d\sigma}{dt}(t=q'^2))^{1/2}\}^2$$

where

$$q'^0 = k^0 - q^0 - E_t$$

$$\vec{q}' = \vec{k} - \vec{q} - \vec{p}_t \tag{24}$$

with $(k^0, \vec{k})$ the momentum of the incoming ^3He.

For the imaginary part of the $^3He^*$ selfenergy of eq. (23) we take

$$Im\ \Sigma_{He^*} = -\frac{1}{2}\sigma_{He-N}\,\rho\, v_{rel} \tag{25}$$

where $v_{rel} = \frac{k}{E_{He}(k)}, \rho$ is the nuclear density and σ_{He-N} is the total cross section for the $N + {}^3He \longrightarrow X$ reaction. Eq. (23) has been derived by assuming a closure sum over all intermediate He, He^* states and subtracting the contribution of the intermediate state where one has the ${}^3He$ in its ground state.

To estimate the average value of the intermediate excited states energy, we evaluate explicitly the form factors appearing in the calculations of the differential cross section of the process depicted in fig. 4,

$$< \psi_{1s}|e^{-i\vec{q}'\vec{x}}|\psi_n >, < \psi_n|e^{-i\vec{q}\vec{x}}|\psi_{1s} > \tag{26}$$

where ψ_{1s} and ψ_n are the wave functions of the ${}^3He$ in the ground state and in the n excited state.

If we take a plane wave with momentum $\vec{p}$ for the wave function ψ_n, we can calculate analytically such form factors getting

$$< \psi_{1s}|e^{-i\vec{q}'\vec{x}}|\psi_n > \sim e^{-(\vec{p}-\vec{q}')/2\alpha^2} \tag{27}$$

with the same α as in eq. (13). (Notice that the former expressions are calculated in the framework where the ${}^3He$ is at rest).

We take for $\vec{p}$ the value that maximizes the product of the two form factors, getting

$$\vec{p} = \frac{1}{2}(\vec{q}' - \vec{q}) \tag{28}$$

In the lab frame, where the ${}^3He$ moves with momentum $\vec{k}$, we can write for the average energy of the excited states

$$\bar{E}^*_{He} = \frac{2}{3}E_{He}(\vec{k}) + E'_N \tag{29}$$

where

$$E_{He}(\vec{k}) = \sqrt{M^2_{He} + \vec{k}^2}$$

$$E'_N = \frac{E_{He}(\vec{k})E_N + \frac{1}{2}(\vec{q}' - \vec{q})\vec{k}}{M_{He}} \tag{30}$$

with

$$E_N = \sqrt{M^2 + [\frac{1}{2}(\vec{q}' - \vec{q})]^2} \tag{31}$$

with M the nucleon mass. The process where we excite a t^* instead of ${}^3He$ would give us the same cross section as eq. (23) and is also included.

The probability of this reaction per unit length, needed in the Monte Carlo simulation, is given by eq.(23) omitting the d^3r integration.

3.5 ^3He or t breakup

To exclude the processes where the ^3He breaks, we need the total cross section for the $^3He + N \longrightarrow X$ reaction, that we calculate using an eikonal approximation,

$$\sigma_{He-N}(s) = 2 \int d^2b[1 - e^{-\frac{3}{2}\sigma_{NN}(s_N)\int_{-\infty}^{\infty} dz\rho(\vec{b},z)}] \tag{32}$$

where σ_{NN} is the total NN cross section [17], s the Mandelstam variable of the $^3He - N$ system y s_N the one of the NN system and ρ the ^3He density.

For the $t + N \longrightarrow X$ cross section we also take the eq. (32) due to the isospin symmetry. With this cross section we define a probability per unit length of He o t breakup, $P_b = \sigma_{He-N}(s)\rho(r)$, with $\rho(r)$ the ^{12}C density. Then if step 2) of section 2 happens to occur in the P_b segment the event is dismissed for the reaction. Recall, however, that the possibility of $He(t)$ breakup and recombination is explicitly considered in the former section.

3.6 Coherent pion production

The model for the coherent pion production is fully described in ref. [18]. We will take the results from that reference and add them to the results for the incoherent channels obtained in the simulation.

4 Results and Conclusions

In this section we present the results of the inclusive $^{12}C(^3He,t)$ cross section at $T_{He} = 2GeV$ and zero degrees (see fig. 5).

The curve labeled 8 is the total calculated cross section for the inclusive $^{12}C(^3He,t)$ reaction. One can see that the shift in the apparent Δ peak is reproduced.

The curve 7 represents the contribution of all the incoherent channels (discussed in the previous section) to the inclusive reaction. We can observe in the figure that the sum of all the incoherent channels shifts considerably the strength at higher t energies, but the position of the peak is not much altered.

In the curve 6 we plot the contribution of the coherent pion production channel to the inclusive reaction. The most interesting feature is that the peak of the coherent pion production is considerably shifted (about 70 MeV) with respect to the incoherent one. This feature is partly responsible for the shift of the peak in the total inclusive $(^3He,t)$ cross section, collaborating with the enhancement of the strength at high t energies produced by the incoherent channels.

In the curve 5 we plot the contribution of the incoherent pion production channel to the inclusive reaction. This curve includes all the multistep processes such that the last step is a incoherent pion production. The model

for the π-production processes in the $(^3He,t)$ and $(^3He,^3He)$ reactions includes the DET and DEP mechanisms, the π-N s-wave interaction and also the medium corrections. The incoherent pion production peaks at the same position as the elementary $(^3He,t)$ reaction on the p, something confirmed experimentally [2]. One should note that we do not follow the final state interaction (FSI) of the pions or the nucleons produced. In the spirit of the MC simulation which we use this FSI does not change the inclusive cross section, but it redistributes the strength in different channels. For instance, some of the pions of curve 5 would be absorbed and show up as $2N$ or $3N$ emission. Hence this curve is not directly comparable with the exclusive experiments.

In the curve 4 we plot the contribution of the virtual pion absorption (multinucleon emission). This means that in this curve we include all the contributions from multistep processes such that in the last step there is a virtual pion absorption.

In the curve 1 we plot the contribution of the multistep processes such that in the last step there is a quasielastic $(^3He,t)$ process. We call *one step quasielastic processes* to these ones. The one step quasielastic processes fill the region of very high t energy.

In the curve 2 we plot the contribution of the multistep processes such that in the last step there is a quasielastic (t,t) process. Before this last step a $(^3He,t)$ reaction necessary took place. We call *two step quasielastic processes* to these ones.

In the curve 3 we plot the contribution of the quasielastic processes with intermediate He(t) break up. This means that in this curve we include all the contributions from multistep processes such that in the last step there is a $He(t)$ break up followed by recombination to give a t.

The classification of events in fig. 5 is done, as we have discussed, in base to the last step in the MC simulation. This means that, for instance, two step processes in incoherent pion production where the pion is produced in the first step are not included in curve 5, but would be counted in some other curve. However, we have checked that these two step processes give a small contribution and hence the association of curve 5 to pion production in any step is already a very good approximation. The same can be said for other channels.

One of the interesting findings in fig. 5 is the fact that the contribution from virtual pion absorption (requiring at least two nucleons) peaks at excitation energies close to the pion mass. We commented on that in sect. 3.2 and gave there qualitative reasons for it. It is very interesting to note that the shape of this distribution is very similar to the $2p$ emission in the $(^3He,t)$ reaction on the deuteron [2]. The experimental observation of a shift of the $2p$ emission distribution in ^{12}C to higher excitation energies [2] would find a qualitative interpretation, to the light of the present results, in the fact that due to FSI some of the real pions of curve 5 would be absorbed and the corresponding strength of this process would peak at the same position of curve 5. The proportion of this pion reabsorption obviously grows with the nuclear mass.

In summary, we have observed that the inclusive $(^3He, t)$ reaction in nuclei is a very involved process. We have tackled the reaction looking at all the channels which can give a contribution to the inclusive cross section, and have shown that many of them are partly responsible for the large shift of strength to higher t energies, as observed in the experiment. The coherent pion production channel played an important role in the shift of the peak position.

While former analyses of the process have made emphasis on the delta properties in the nuclear medium, we have shown that some of the peculiar features of this reaction are not tied to the Δ nuclear dynamics, and quasielastic scattering, non resonant pion absorption, etc... are also relevant to the process.

Acknowledgements

This work was partially supported by CICYT, contract AEN 93-1205.

References

[1] J. Chiba et al., Phys. Rev. Lett. 67 (1991) 1983.

[2] T. Hennino et al., Phys. Lett. B 283 (1992) 42.

[3] E. Oset, E. Shiino and H. Toki, Phys. Lett. B 224 (1989) 249.

[4] T. Udagawa, S.H. Hong and F. Osterfeld, Phys. Lett. B245 (1990) 1.

[5] J. Delorme and P.A.M. Guichon, Phys. Lett. B263 (1991) 15 7.

[6] P. Oltmanns, F. Osterfeld and T. Udagawa, Phys. Lett. B299 (1993) 194.

[7] E. Oset, P. Fernández de Córdoba, J. Nieves and M.J. Vicente-Vacas, Phys. Scr. 48 (1993) 101.

[8] V. F. Dimitriev, Phys. Rev. C48 (1993) 357.

[9] T. Hennino et al. Phys. Lett. B303 (1993) 236.

[10] J. Chiba, Talk at the Int. Workshop on deltas in nuclei, Riken (Tokyo), May 1993.

[11] P. Fernández de Córdoba and E. Oset, Nucl. Phys. A544 (1992) 793.

[12] L.L. Salcedo et al. Nucl. Phys. A484 (1988) 557.

[13] N.P. Goldstein et al., Can. J. Phys. 48(1970)2629. H. Langevin-Joliot et al., Nucl. Phys. A518(1970)309. R. Frascaria et al., Phys. Lett. 66B(1977)329. M. Blecher et al., Phys. Rev. Lett. 24(1970)1126. J. Fain et al., Nucl. Phys. A262(1976)413. G.D. Alkhazov et al., Phys. Lett. 85B(1979)43. W.T.H. Van Oers, private communication. D.K. Hasell, private communication.

[14] E. Oset and D. Strottman. Nucl. Phys. A355 (1981) 437.

[15] J.M. Nieves, E. Oset, C. García Recio, Nucl. Phys. A554 (1993) 509; ibid. pag. 554.

[16] E. Oset,P. Fernández de Córdoba, L.L. Salcedo and R. Brockman, Phys. Reports 188 (1990) 79.

[17] J. Cugnon, private communication.

[18] P. Fernández de Córdoba, J. Nieves, E. Oset and M.J. Vicente-Vacas Phys. Lett. B319 (1993) 416.

[19] C. Gaarde, Nucl. Phys. A478 (1988) 475c.

Figure Captions

Fig. 1:
Double differential cross section for $(^3He, t)$ on different target nuclei as a function of the t kinetic energy. Data from ref. [19]

Fig. 2:
$^3He + N \rightarrow t + N$ collision in the lab system.

Fig. 3:
^3He–selfenergy diagrams associated to the two (a) and three (b) nucleons emission process with t as intermediate state.

Fig. 4:
Diagrammatic representation of the process (22) with an excited helium – $^3He^*$– as intermediate state.

Fig. 5:
Contributions to the cross section for the $(^3He, t)$ inclusive reaction on ^{12}C.
(1) Quasielastic $^3He + N \rightarrow t + N$.
(2) Two step quasielastic $^3He + N \rightarrow ^3He(t) + N$ followed by $^3He(t) + N' \rightarrow t + N'$.
(3) Two step quasielastic scattering with intermediate He(t) break up: $^3He + N \rightarrow ^3He^*(t^*) + N$ followed by $^3He^*(t^*) + N' \rightarrow t + N'$.
(4) Virtual pion production followed by pion absorption.
(5) Incoherent pion production.
(6) Coherent pion production.
(7) Sum of incoherent processes 1–5.
(8) Total: sum of coherent and incoherent processes.
Data from ref.[19]

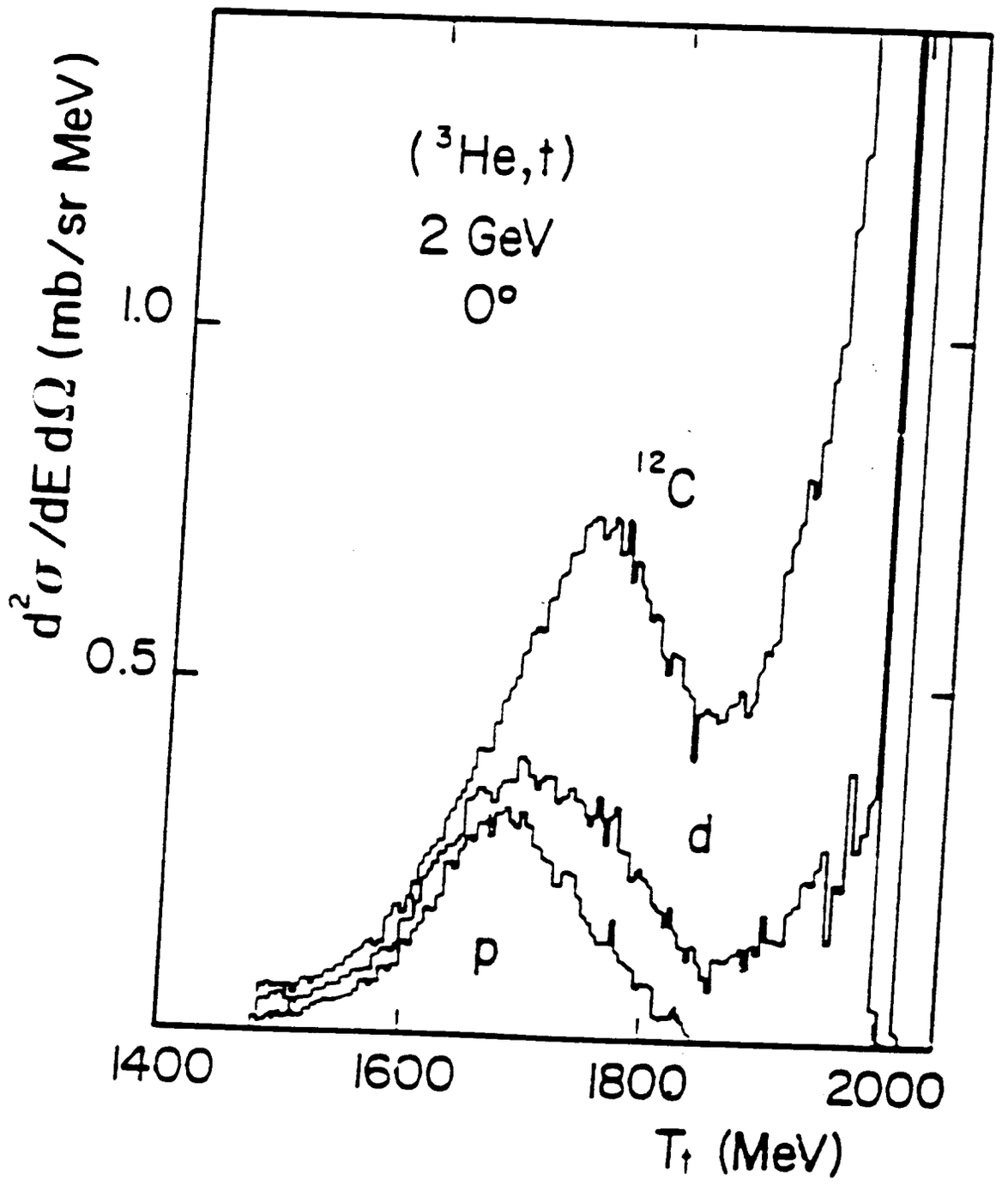
$d^2\sigma/dE\,d\Omega$ (mb/sr MeV)
1.0
0.5
(^{3}He,t)
2 GeV
0°
^{12}C
d
p
1400
1600
1800
2000
T_t (MeV)

Fig 1

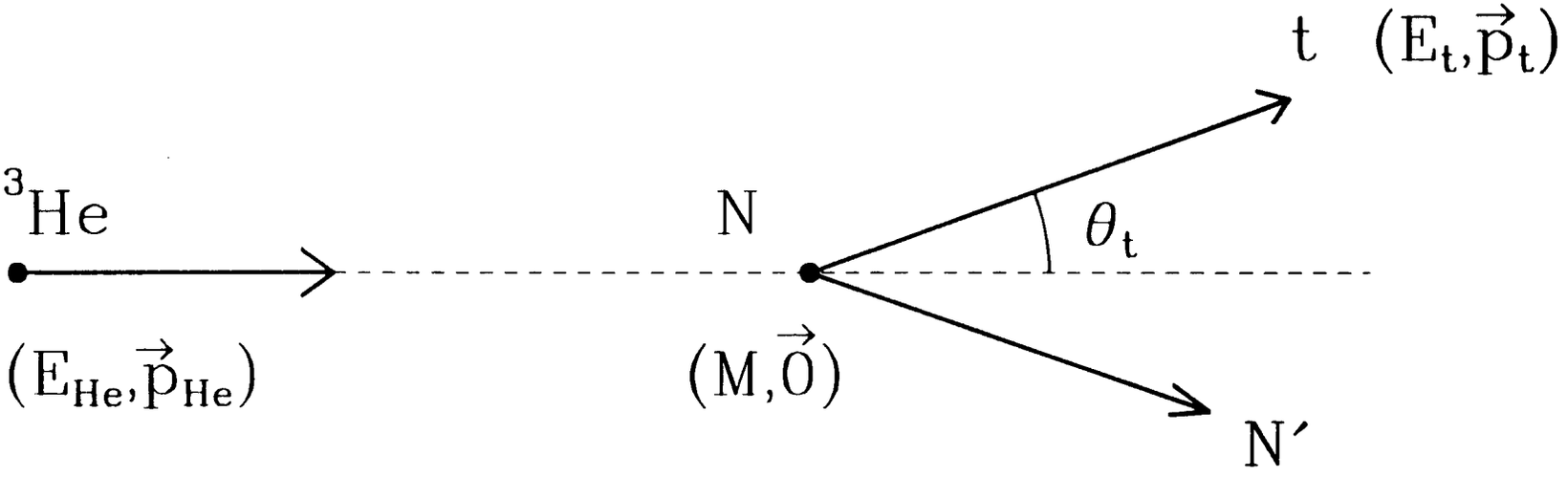

Fig. 2

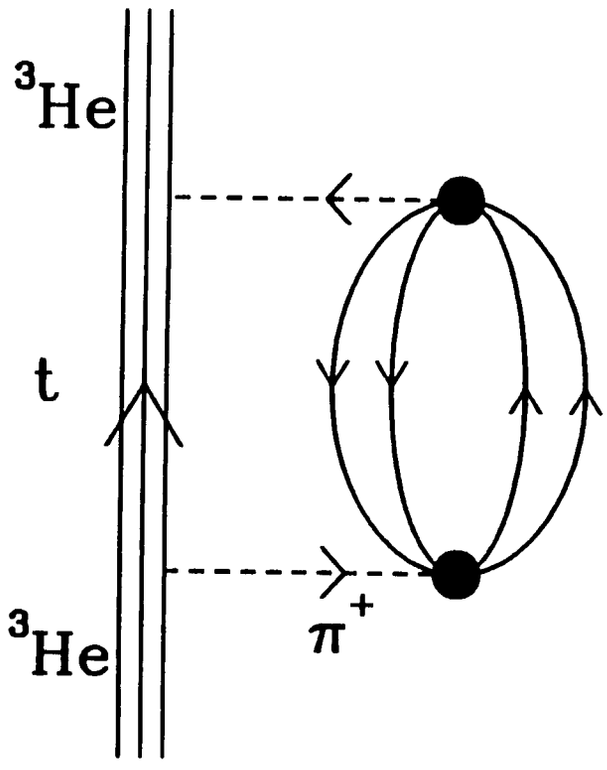

a)

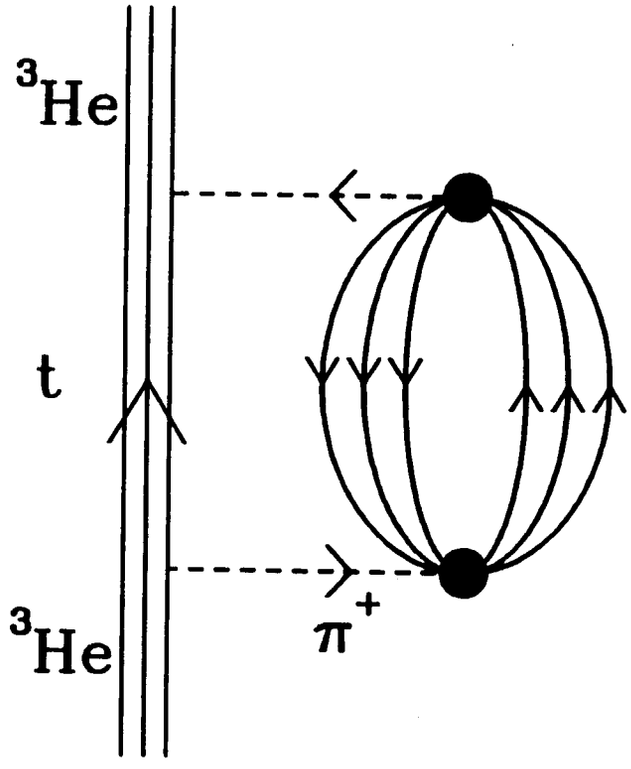

b)

Fig. 3

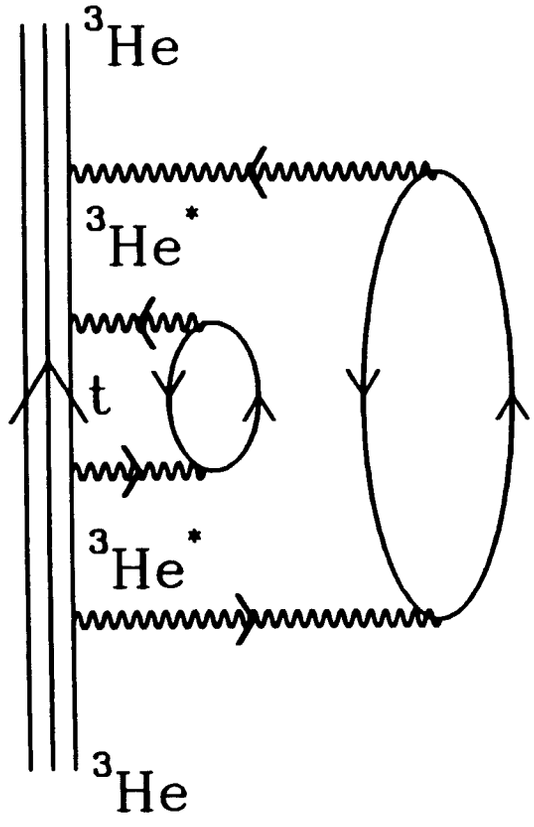

Fig 4

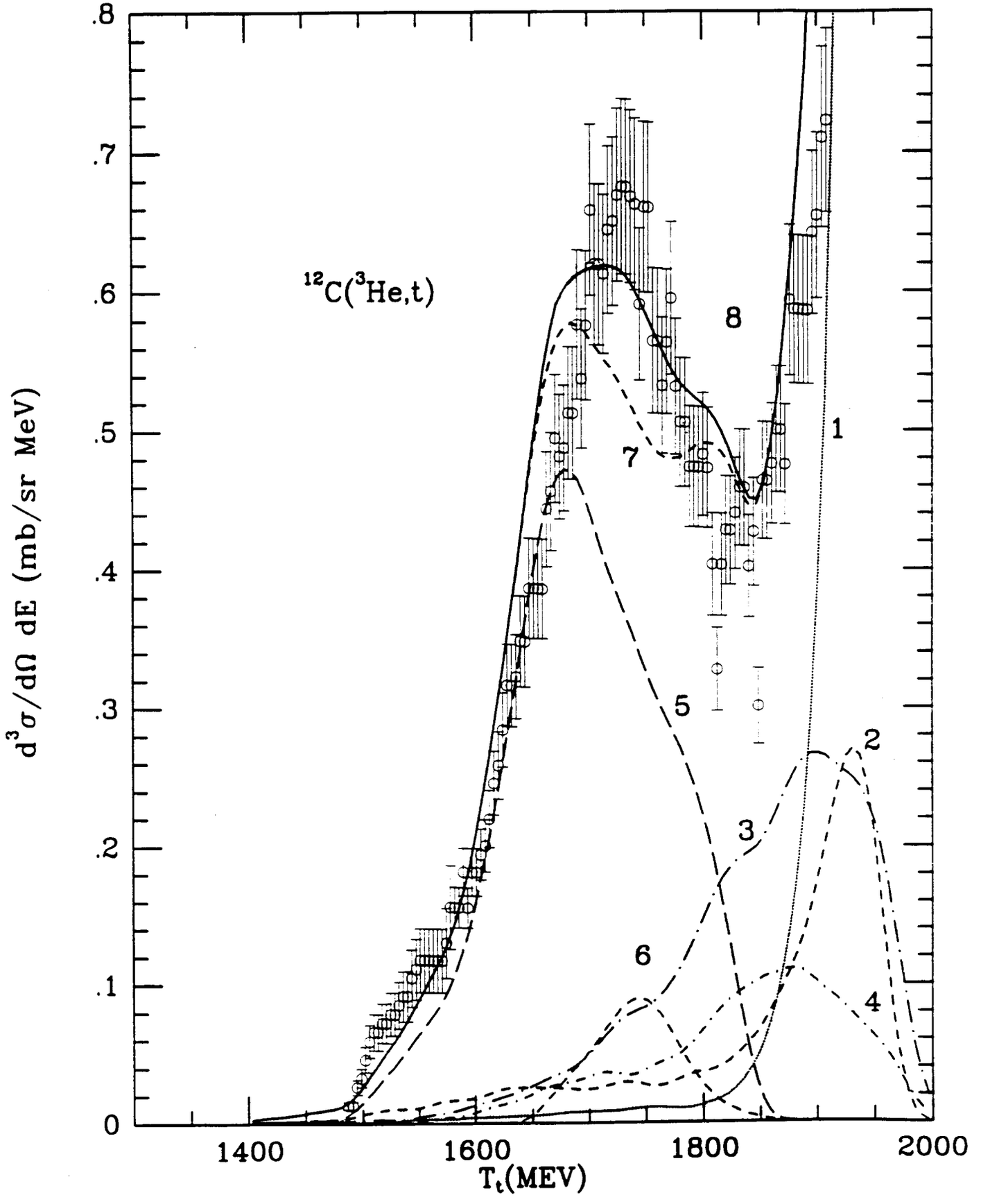
$^{12}C(^3He,t)$
$d^3\sigma/d\Omega\ dE$ (mb/sr MeV)
T_t(MEV)
0
.1
.2
.3
.4
.5
.6
.7
.8
1400
1600
1800
2000
1
2
3
4
5
6
7
8

Fig. 5